AIP | Applied Physics Letters

The influence of growth conditions on carrier recombination mechanisms in 1.3μm GaAsSb/GaAs quantum well lasers

N. Hossain, K. Hild, S. R. Jin, S.-Q. Yu, S. R. Johnson et al.

Citation: Appl. Phys. Lett. **102**, 041106 (2013); doi: 10.1063/1.4789859
View online: http://dx.doi.org/10.1063/1.4789859
View Table of Contents: http://apl.aip.org/resource/1/APPLAB/v102/i4
Published by the AIP Publishing LLC.

The influence of growth conditions on carrier recombination mechanisms in 1.3 μm GaAsSb/GaAs quantum well lasers

N. Hossain,[1] K. Hild,[1] S. R. Jin,[1] S.-Q. Yu,[2,3] S. R. Johnson,[2] D. Ding,[2] Y.-H. Zhang,[2] and S. J. Sweeney[1,a)]

[1]*Advanced Technology Institute and Department of Physics, University of Surrey, Guildford, Surrey GU2 7XH, United Kingdom*
[2]*School of Electrical, Computer, and Energy Engineering, Arizona State University, Tempe, Arizona 85287, USA*
[3]*Department of Electrical Engineering, University of Arkansas, Fayetteville, Arkansas 72701, USA*

(Received 13 November 2012; accepted 15 January 2013; published online 28 January 2013)

We investigate the temperature and pressure dependence of the threshold current density of edge-emitting GaAsSb/GaAs quantum well (QW) lasers with different device characteristics. Thermally activated carrier leakage via defects is found to be very sensitive to the growth conditions of GaAsSb QWs. An optimization of the growth conditions reduces the nonradiative recombination mechanisms from 93% to 76% at room temperature. This improvement in carrier recombination mechanisms leads to a large improvement in the threshold current density from 533 Acm^{-2}/QW to 138 Acm^{-2}/QW and the characteristic temperature, T_0 (T_1), from 51 ± 5 K (104 ± 16 K) to 62 ± 2 K (138 ± 7 K) near room temperature. © *2013 American Institute of Physics*. [http://dx.doi.org/10.1063/1.4789859]

Semiconductor lasers emitting at 1.3 μm are of considerable importance to overcome the bandwidth limitation of optical fiber communication systems (OFCS) over relatively short distances, for example, between cities and in metropolitan areas, fiber to the home and local area networks. The conventional InGaAsP/InP quantum well (QW) material system used to make such lasers suffers from poor temperature characteristics resulting in the need to incorporate sophisticated temperature control electronics into the package, leading to a large increase in cost.[1] Moreover, due to the lack of lattice matching and high refractive index contrast materials to form all-epitaxial distributed Bragg reflectors (DBRs), it is also very difficult to fabricate monolithic vertical cavity surface emitting lasers (VCSELs) in the InP material system.[2] The GaAs-based 1.3 μm GaInNAs QWs[3,4] and 1.3 μm InAs/GaAs quantum dots[5,6] have also been investigated extensively. The performance of such lasers is still far from ideal. GaAsSb/GaAs lasers may offer a solution in the search for an uncooled, thermally stable and cheaper semiconductor lasers for 1.3 μm OFCS.[7,8] GaAs permits the growth of near lattice-matched GaAs/AlGaAs DBRs, which have superior optical and thermal properties when compared to other III-V DBRs.[9,10] Furthermore, the fabrication of GaAs based 1.3 μm VCSELs can take full advantage of the industrial standard 850 nm VCSEL fabrication technology, which is attractive from a manufacturing point of view.[11–13] However, the optimization of the growth conditions to grow high-quality $GaAs_{1-x}Sb_x$/GaAs ($x = 0.3$ necessary for ~1.3 μm emission) QW active material is one of the major challenges to make this material system commercially viable.[14–16] The aim of this letter is to compare device characteristics of $GaAs_{1-x}Sb_x$/GaAs QW lasers to aid in the design and optimization of GaAsSb/GaAs-based edge-emitting lasers and VCSELs.

The devices in this study were grown using solid source molecular beam epitaxy (MBE) growth technique under similar growth conditions. We note that VCSELs are more typically grown by the metal organic chemical vapor deposition (MOCVD) growth technique. However, the growth temperature is an important parameter and the optimal temperature for mixed group-V's depends on the composition and the composition for a given As/Sb flux ratio depends on growth temperature for a given set of fluxes, making the optimization process difficult. Another important factor is the level of impurities such as oxygen on the growing surface, which also affects the optimal growth temperature. MBE systems with lower background impurities (compared to MOCVD) in general grow higher quality material and with more control compared to MOCVD grown devices.[9,17] For this reason, MBE has been more widely investigated to grow Sb-based materials. The grown structures consist of a triple $GaAs_{0.9}P_{0.1}$/GaAs/$GaAs_{0.7}Sb_{0.3}$/GaAs/$GaAs_{0.9}P_{0.1}$ (9 nm/5 nm/7 nm/5 nm/9 nm) strain compensated QW active region grown at 495 °C (device A) and 490 °C (device B). The $GaAs_{0.9}P_{0.1}$ strain compensating layers allows growing the maximum number of highly strained QWs and reduces strain driven in-plane Sb segregation.[8] The active region in each device is sandwiched between two 20 nm $Al_{0.25}Ga_{0.75}As$ layers, two 150 nm graded-index AlGaAs layers, one 2 μm *n*-type $Al_{0.65}Ga_{0.35}As$ cladding layer followed by 500 nm GaAs buffer layer at the bottom, and one 2 μm *p*-type $Al_{0.65}Ga_{0.35}As$ cladding layer followed by a 100 nm GaAs cap layer at the top. The broad-area edge-emitting lasers were processed by defining 50 and 100 μm wide ridges. Ti/Pt/Au *p*-contact stripes ranging from 2 to 32 μm and AuGe/Ni/Au *n*-metal contacts were deposited. Further details of the growth and processing of these devices can be found in Ref. 8. The devices were measured as-cleaved.

a)Author to whom correspondence should be addressed. Electronic address: s.sweeney@surrey.ac.uk.

Temperature dependent measurements over the range of 60–300 K were performed by using a standard closed-cycle cryostat set-up. The emission wavelengths (at room temperature (RT)) of devices A and B are found to be very similar at ~1.27 μm and ~1.26 μm, respectively. However, the measured lowest threshold current density (J_{th}) of device B is ~138 Acm^{-2}/QW at RT, which is significantly lower than that of device A (~533 Acm^{-2}/QW). Fig. 1 shows the T_0 (derived from $1/T_0 = d\ln J_{th}/dT$) for device A to be 77 ± 3 K at 200 K compared with $T_0 = 230 \pm 5$ K for device B. T_0 drops to 51 ± 5 K (device A) and 62 ± 2 K (device B) at RT. T_0 (at RT) in these devices is approximately the same as that of conventional InGaAsP/InP devices (typically ~50–60 K near RT[15]). Similar to T_0, we find that T_1 (derived from $1/T_1 = -d\ln\eta_d/dT$) for device A (device B) is 508 ± 11 K (636 ± 4 K) at 200 K, which drops to 104 ± 16 K (138 ± 7 K) at RT. Indeed, when compared with ~1.2 μm InGaAs/GaAs devices, T_1 is significantly lower in these devices.[18] The lower T_1 is an indication of thermally activated recombination processes,[19] which may occur in these lasers at higher temperatures. However, both T_0 and T_1 for device B are higher than that for device A over the temperature range studied, which is consistent with the reduced J_{th} of device B than that of device A. A non-ideal internal quantum efficiency (η_i) may also contribute to the low T_1 values in these devices. The inverse of differential quantum efficiency (η_d) against the cavity length (L_{cav}) was measured from which η_i and internal optical loss (α_i) of device B were determined (using the relation mentioned in Ref. 20) to be 76 ± 1% and 12 ± 0.3 cm^{-1}, respectively. We could not compare the values of these parameters of device B with device A due to the unavailability of multiple cavity length devices. We note that the η_i is lower and α_i is higher in device B (which is showing improved performance in this work) than that of other GaAs-based materials (for which internal quantum efficiency and internal optical loss are 83%-85%[21] and 10 cm^{-1},[22] respectively). The low η_i and high α_i in device B is consistent with the large threshold current density in these devices compared to other GaAs-based lasers, which operate at similar wavelengths for which J_{th}/QW ~ 100 Acm^{-2}.[23] Achieving an ideal QW laser operation in $GaAs_{1-x}Sb_x$/GaAs material system therefore requires an understanding of the important carrier recombination mechanisms.

Fig. 2 shows the normalized (at T = 60 K) temperature dependence of J_{th} and its radiative component (J_{rad}), which is extracted from the pinning level of the measured integrated spontaneous emission at laser threshold (further details of spontaneous emission measurement technique can be found in Ref. 24). Here, J_{rad} is determined by assuming that (a) J_{rad} is proportional to the integrated spontaneous emission rate at laser threshold and (b) that non-radiative recombination is negligible at the lowest temperature. J_{rad} therefore provides a measure of the maximum radiative component of J_{th} as a function of temperature. From the measured J_{th} and J_{rad}, for device B, we estimate that the relative ratio of the radiative and non-radiative currents to J_{th} are ~24% and ~76%, respectively, at RT, compared with ~7% and ~93% for device A. Thus, a non-radiative recombination process dominates J_{th} at RT in both structures. It can also be seen that in addition to having a lower absolute J_{th}, device B has a higher J_{rad}/J_{th} than in device A. A photoluminescence study of $GaAs_{0.7}Sb_{0.3}$/GaAs QW lasers (similar to devices A and B) suggests that antimony segregation causes lower photoluminescence intensity and a larger full-width at half maximum and hence a higher J_{th}.[8] Antimony segregation introduces defects at the GaAsSb active region—GaAs spacer interface forming a thermally activated loss mechanism as more energetic carriers increasingly recombine via the defect states. It follows that the lower growth temperature of device B reduces Sb segregation and the associated defect density and consequently reduces the thermally activated non-radiative processes, thereby reducing J_{th} for device B. It is important to maintain the improved growth conditions for repeated growths. The active material mole fraction must be continually and accurately calibrated to maintain the desired mole fraction and the substrate to substrate thermal couple temperature offset must be calibrated every run so that the temperature is controlled within a few degrees Celsius run to run. This can be done using pyrometry or band edge thermometry. We note that while the growth temperature of GaAsSb QWs offers a possible explanation of the reduced J_{th} of device B, this in itself is insufficient. Others factors, such as

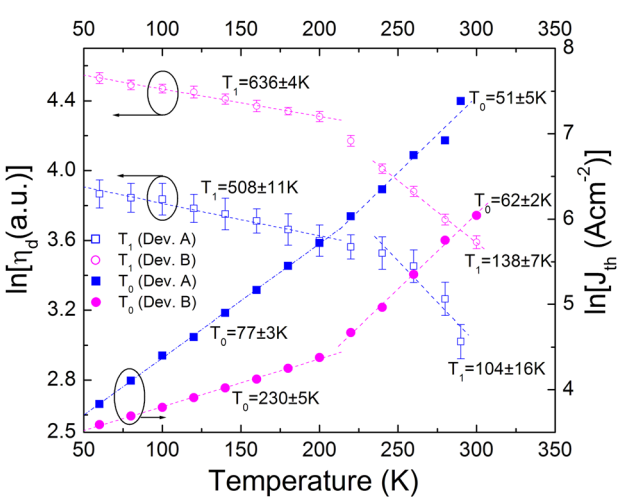

FIG. 1. ln[I_{th}] and ln[η_d] as a function of temperature.

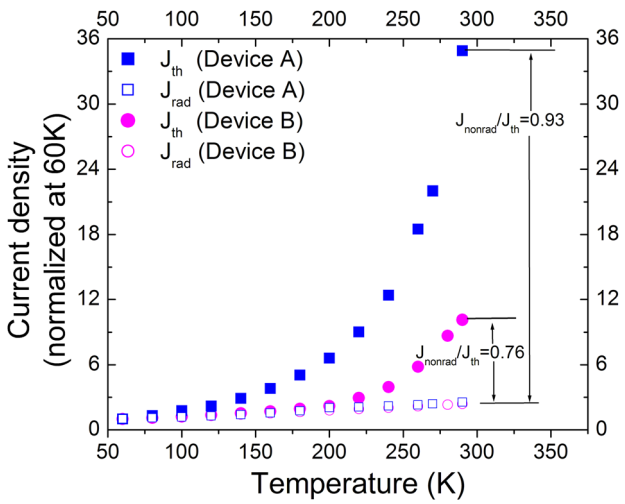

FIG. 2. Normalized (at $T = 60$ K) temperature dependence of J_{th} (full squares and circles). Temperature dependence of J_{rad} (open squares and circles).

device processing may also has affected the performance of these devices, which remains the subject of further investigation. We also note that the presence of defects in these devices suggests that the analysis in Fig. 2 may overestimate J_{rad} at low temperature due to there being another non-radiative path active at low temperature. Considering this non-radiative path (at 60 K) in our analysis, the non-radiative contribution at RT in device A and device B will be higher than ~76% and ~93%, respectively. However, due to the higher defect density in device A, non-radiative contribution at RT in device A compared to device B will be even higher than the estimated values in Fig. 2. Hence, the possible overestimation of J_{rad} in Fig. 2 does not affect our current analysis and conclusions.

To further probe the recombination mechanisms, high pressure techniques were utilized. The application of hydrostatic pressure mainly affects the conduction band (CB) causing an increase in the direct band gap of III–V semiconductors and is therefore an ideal method to investigate the important band gap dependent non-radiative processes (like Auger, carrier leakage, and defect-related recombination). With increasing pressure, the Auger recombination process reduces, carrier leakage mechanisms increase or remain stable, and defect related recombination remains constant. Further details of these dependencies can be found in Ref. 25. Fig. 3 shows the measured pressure dependence of threshold current (normalized at 0 kbar) at RT. Also shown is the ideal expected variation of $J_{rad} \propto E_g^2$,[26] where E_g is the bandgap (taken from $E_g = hc/\lambda$, where λ is the measured lasing wavelength). It can be clearly seen that the threshold current increases with pressure much faster than J_{rad} for both devices A and B, which confirms that the lasers are not operating in a radiatively dominated regime. J_{th} for devices A and B increase by ~27% and ~44%, respectively, up to 7 kbar at RT suggesting the presence of carrier leakage in these devices as observed earlier in similar devices.[1,15,16] The lower rate of increase in J_{th} with pressure in device A compared to device B may be due to the higher growth temperature of device A, which increases Sb segregation and thus the concentration of defects. The fact that J_{th} for device A has a stronger temperature dependence but weaker pressure dependence indicates the presence of defects which are shallow and therefore not pressure dependent.

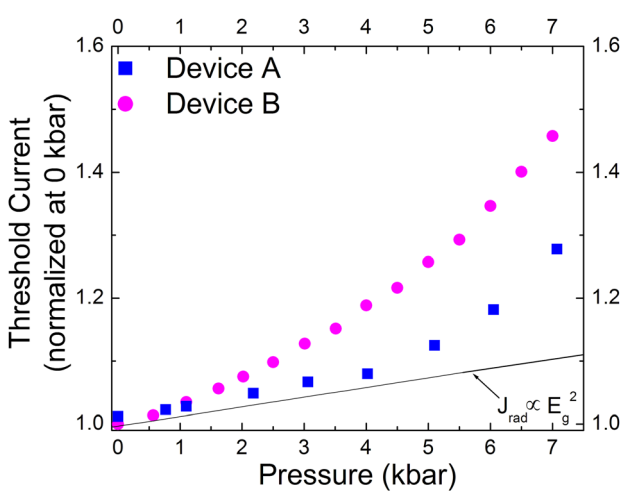

FIG. 3. Measured pressure dependence of threshold current and ideal J_{rad} at RT.

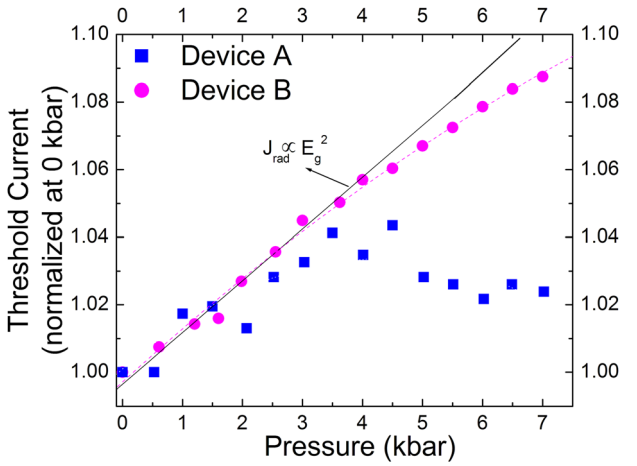

FIG. 4. Measured pressure dependence of threshold current and ideal J_{rad} at 120 K.

Fig. 4 shows the measured pressure dependence of threshold current (normalized at 0 kbar) at 120 K. It can be seen that the threshold current of device B increases with increasing pressure at the similar rate to J_{rad}, indicating that radiative recombination dominates at this low temperature. A slight deviation of threshold current from $J_{rad} \propto E_g^2$ may be due to a couple of factors. A weak type-I conduction band alignment with a conduction band offset, $\Delta E_c = 19.0 \pm 19.1$ meV, has been reported at the $GaAs_{0.7}Sb_{0.3}$/GaAs interface of these materials,[27] as shown in Fig. 5. Pressure coefficients for the band gap for both devices A and B are measured to be ~7.7 meV/kbar. On the other hand, the well known pressure co-efficient of GaAs is 10.7 meV/kbar.[1] Hence, with increasing pressure, ΔE_c increases at a rate of ~3 meV/kbar if we assume that hydrostatic pressure predominantly affects the conduction band[28,29] and forms a stronger type-I band alignment at the $GaAs_{0.7}Sb_{0.3}$/GaAs interface (inset of Fig. 5), which increases the electron-hole overlap. As a result, lower carrier injection is required to achieve the required gain. The

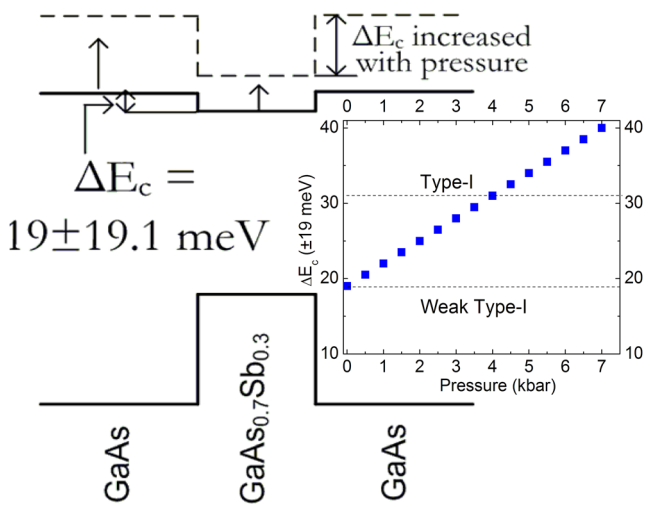

FIG. 5. Band alignment at $GaAs_{0.7}Sb_{0.3}$/GaAs interface. With increasing pressure, ΔE_c increases and forms a type-I band alignment at the $GaAs_{0.7}Sb_{0.3}$/GaAs interface (inset).

reduction of threshold carrier density (n_{th}) with pressure will decrease J_{rad}, which would cause J_{rad} deviate from the simple $J_{rad} \propto E_g^2$ model as described in Ref. 30. Furthermore, the presence of Auger recombination may also give rise to a lower pressure dependence of threshold current, as has been observed previously in Ref. 1.

In summary, it is found that the threshold current of $GaAs_{1-x}Sb_x/GaAs$ QW lasers is dominated by non-radiative recombination mechanisms which are responsible for the poor temperature sensitivity of the devices resulting in low T_0 and T_1 values at RT. Pressure dependence measurements suggest that carrier leakage mechanism dominates the threshold current density at room temperature in these devices. Thermally activated carrier leakage via defects is found to be very sensitive to the growth conditions of QWs. Optimization of growth conditions leads to an improvement in the radiative recombination process from ~7% to ~24%, results a lower J_{th} from 533 Acm^{-2}/QW to 138 Acm^{-2}/QW and a higher T_0 from 51 ± 5 K to 62 ± 2 K at RT. Optimization of 1.3 μm $GaAs_{1-x}Sb_x/GaAs$ QW lasers will rely upon reducing the thermally activated carrier leakage via the defect states and by careful optimization of growth conditions.

The authors gratefully acknowledge the EPSRC (UK), grants GR/T21516/1 and EP/H005587/1, the Royal Academy of Engineering, and the Kwan Trust Fund in supporting this work.

[1]K. Hild, S. J. Sweeney, S. Wright, D. A. Lock, S. R. Jin, I. P. Marko, S. R. Johnson, S. A. Chaparro, S.-Q. Yu, and Y.-H. Zhang, Appl. Phys. Lett. **89**, 173509 (2006).
[2]W. Braun, P. Dowd, C. Z. Guo, S. L. Chen, C. M. Ryu, U. Koelle, S. R. Johnson, Y. H. Zhang, J. W. Tomm, T. Elsasser, and D. J. Smith, J. Appl. Phys. **88**, 3004 (2000).
[3]S. R. Jin, S. J. Sweeney, S. Tomić, A. R. Adams, and H. Riechert, Appl. Phys. Lett. **82**, 2335 (2003).
[4]A. D. Andreev and E. P. O'Reilly, Appl. Phys. Lett. **84**, 1826 (2004).
[5]Y. Qiu, P. Gogna, S. Forouhar, A. Stintz, and L. F. Lester, Appl. Phys. Lett. **79**, 3570 (2001).
[6]I. P. Marko, A. R. Adams, S. J. Sweeney, D. J. Mowbray, M. S. Skolnick, H. Y. Liu, and K. M. Groom, IEEE J. Sel. Top. Quantum Electron. **11**, 1041 (2005).
[7]P. Dowd, W. Braun, D. J. Smith, C. M. Ryu, C.-Z. Guo, S. L. Chen, U. Koelle, S. R. Johnson, and Y.-H. Zhang, Appl. Phys. Lett. **75**, 1267 (1999).
[8]S.-Q. Yu, D. Ding, J.-B. Wang, N. Samal, X. Jin, Y. Cao, S. R. Johnson, and Y.-H. Zhang, J. Vac. Sci. Technol. B **25**, 1658 (2007).
[9]M. S. Noh, R. D. Dupuis, D. P. Bour, G. Walter, and N. Holonyak, Appl. Phys. Lett. **83**, 2530 (2003).
[10]J. J. Wierer, D. A. Kellogg, and N. Holonyak, Appl. Phys. Lett. **74**, 926 (1999).
[11]M. Dinu, J. E. Cunningham, F. Quochi, and J. Shah, J. Appl. Phys. **94**, 1506 (2003).
[12]M. J. Cherng, G. G. Stringfellow, and R. M. Cohen, Appl. Phys. Lett. **44**, 677 (1984).
[13]Y.-K. Su, C.-T. Wan, R. W. Chuang, C.-Y. Huang, W. C. Chen, Y. S. Wang, and H.-C. Yu, J. Cryst. Growth **310**, 4850 (2008).
[14]C.-A. Chang, R. Ludeke, L. L. Chang, and L. Esaki, Appl. Phys. Lett. **31**, 759 (1977).
[15]N. Hossain, S. R. Jin, S. J. Sweeney, S.-Q. Yu, S. R. Johnson, D. Ding, and Y. H. Zhang, Proc. SPIE **7616**, 761608 (2010).
[16]N. Hossain, K. Hild, S. J. Sweeney, S.-Q. Yu, S. R. Johnson, D. Ding, and Y. H. Zhang, in *Proceedings of IEEE Photonics Global Conference Singapore* (IEEE, 2010), pp. 1–3.
[17]S.-W. Ryu, and P. D. Dapkus, Electron. Lett. **38**, 564 (2002).
[18]N. Tansu, Y.-L. Chang, T. Takeuchi, D. P. Bour, S. W. Corzine, M. R. T. Tan, and L. J. Mawst, IEEE J. Quantum Electron. **38**, 640 (2002).
[19]N. Hossain, S. R. Jin, S. Liebich, M. Zimprich, K. Volz, B. Kunert, W. Stolz, and S. J. Sweeney, Appl. Phys. Lett. **101**, 011107 (2012).
[20]S. J. Sweeney and A. R. Adams, "Optoelectronic devices and materials," in *Springer Handbook of Electronic and Photonic Materials* (Springer, 2006).
[21]X. D. Wang, S. M. Wang, Y. Q. Wei, M. Sadeghi, and A. Larsson, Electron. Lett. **40**, 1338 (2004).
[22]Y. Q. Ning, Y. F. Sung, Z. H. Jin, and L. J. Wang, Proc. SPIE **5644**, 614 (2005).
[23]G. Adolfsson, S. M. Wang, M. Sadeghi, and A. Larsson, Electron. Lett. **43**, 454 (2007).
[24]S. J. Sweeney, A. F. Philips, A. R. Adams, E. P. O'Reilly, and P. J. A. Thijs, IEEE Photonics Technol. Lett. **10**, 1076 (1998).
[25]K. Hild, S. J. Sweeney, I. P. Marko, S. R. Jin, S. R. Johnson, S. A. Chaparro, S.-Q. Yu, and Y.-H. Zhang, Phys. Status Solidi B **244**, 197 (2007).
[26]A. R. Adams, M. Silver, and J. Allam, Semicond. Semimetals **55**, 301 (1998).
[27]S. R. Johnson, C. Z. Guo, S. Chaparro, Yu. G. Sadofyev, J. Wang, Y. Cao, N. Samal, J. Xu, S. Q. Yu, D. Ding, and Y.-H. Zhang, J. Cryst. Growth **251**, 521 (2003).
[28]C. G. Van de Walle and M. M. Martin, Phys. Rev. B **35**, 8154 (1987).
[29]N. Hossain, I. P. Marko, S. R. Jin, K. Hild, S. J. Sweeney, R. B. Lewis, D. A. Beaton, and T. Tiedje, Appl. Phys. Lett. **100**, 051105 (2012).
[30]N. F. Masse, A. R. Adams, and S. J. Sweeney, Appl. Phys. Lett. **90**, 161113 (2007).